REPORT DOCUMENTATION PAGE

Form Approved
OMB No. 0704-0188

1. REPORT DATE *(DD-MM-YYYY)*	2. REPORT TYPE	3. DATES COVERED *(From - To)*
30-09-2016	Performance / Technical Report (Quarterly)	7/1/16 - 9/30/16

4. TITLE AND SUBTITLE
A Hybrid Approach to Composite Damage and Failure Analysis Combining Synergistic Damage Mechanics and Peridynamics

5a. CONTRACT NUMBER

5b. GRANT NUMBER
N00014-16-1-2173

5c. PROGRAM ELEMENT NUMBER

6. AUTHOR(S)
Dr. Ramesh Talreja

5d. PROJECT NUMBER

5e. TASK NUMBER

5f. WORK UNIT NUMBER

7. PERFORMING ORGANIZATION NAME(S) AND ADDRESS(ES)
Texas A&M Engineering Experiment Station (TEES)
1470 William D Fitch Pkwy
College Station, TX 77845-4645

8. PERFORMING ORGANIZATION REPORT NUMBER
M1601473 / 505170-00001/2

9. SPONSORING/MONITORING AGENCY NAME(S) AND ADDRESS(ES)
Office of Naval Research
875 N. Randolph Street, Suite 1425
Arlington, VA 22203-1995

10. SPONSOR/MONITOR'S ACRONYM(S)
ONR

11. SPONSOR/MONITOR'S REPORT NUMBER(S)

12. DISTRIBUTION/AVAILABILITY STATEMENT
unlimited

13. SUPPLEMENTARY NOTES

14. ABSTRACT
The work performed in the reporting period has been focused on continuation of Task 1.1 and Task 2.1 described in the project proposal. The activities related to Task 1.1 area computational micromechanics failure analysis of a representative volume element containing disordered fiber distributions. Procedures have been developed to simulate formation of fiber clusters during resin infusion in polymer matrix composites. Task 2.1 is concerned with damage evolution in a peridynamic model of poroelastic materials. Effects of porosity level and of the presence of notches (short and long) have been studied. Ongoing work in both tasks is outlined.

15. SUBJECT TERMS
Computational micromechanics, Cavitation induced cracking, Peridynamics, Porous media

16. SECURITY CLASSIFICATION OF: a. REPORT	b. ABSTRACT	c. THIS PAGE	17. LIMITATION OF ABSTRACT	18. NUMBER OF PAGES	19a. NAME OF RESPONSIBLE PERSON
U	U	U	SAR	8	William Nickerson
					19b. TELEPHONE NUMBER *(Include area code)* 703-696-8485

Standard Form 298 (Rev. 8/98)
Prescribed by ANSI Std. Z39.18

Quarterly Progress Report, July 1 – September 30, 2016

A Hybrid Approach to Composite Damage and Failure Analysis Combining Synergistic Damage Mechanics and Peridynamics

Award Number N00014-16-1-2173

DOD – NAVY – Office of Naval Research

PI: Ramesh Talreja
Co-PI: Florin Bobaru

Executive Summary

The work performed in the reporting period has been focused on continuation of Task 1.1 and Task 2.1described in the project proposal. The activities related to Task 1.1 are a computational micromechanics failure analysis of a representative volume element containing disordered fiber distributions. Procedures have been developed to simulate formation of fiber clusters during resin infusion in polymer matrix composites. Task 2.1 is concerned with damage evolution in a peridynamic model of poroelastic materials. Effects of porosity level and of the presence of notches (short and long) have been studied. Ongoing work in both tasks is outlined.

Task 1.1 Micro-level crack initiation

Background and motivation

In most manufacturing processes for polymer matrix composites (PMCs) one starts with dry bundles of fibers. On resin infusion, the initially closed-pack fibers are spread out to the degree dictated by the intended fiber volume fraction. Whether the end product is a pre-impregnated layer, or a thick part produced by resin transfer molding (RTM), the configuration in which the fibers finally appear is far from uniform. The final nonuniform distribution of fibers consists of clustered regions and resin pockets. The clustered fiber regions promote formation of debonds, which by connecting with neighboring debonds produce micro-cracks. In this task, the initiation of debonds as a result of cavitation in the polymer matrix close to the fiber surfaces is examined closely. The following results describe the progress made in the reporting period.

Approach and Results

A novel procedure has been devised to create nonuniform fiber distributions from the initial fiber bundle (with representation as a concentric rings of fibers in contact with fibers in the neighboring rings (see Fig. 1.1). The radial distance between the neighboring fibers, r, and the angular separation of fibers (also shown in Fig. 1.1) were varied usinga uniform random distribution. For each combination of these variables, five realizations were generated. The procedure for generating a realization is illustrated in Fig. 1.2.

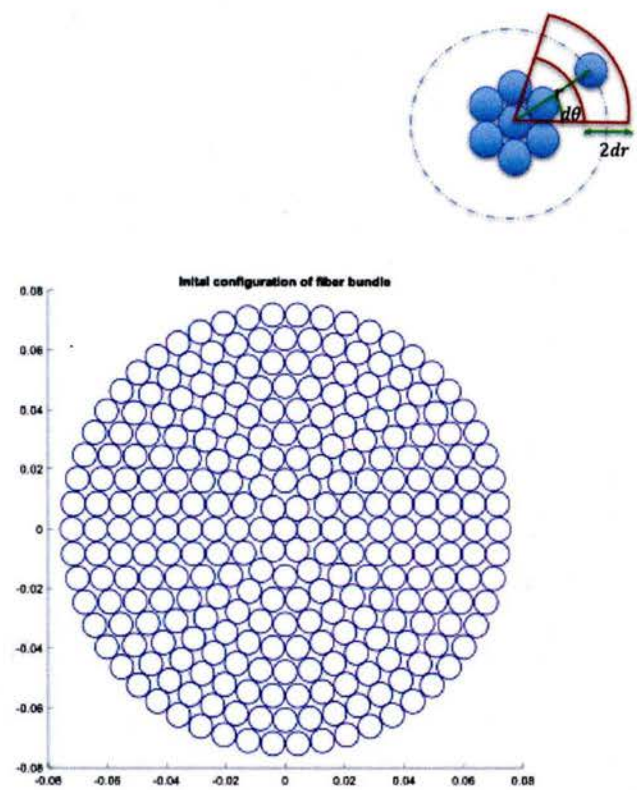

Fig. 1.1. A representative configuration of a dry fiber bundle is displayed in the figure to the left and the top figure shows the two variables r and θ used in simulations to produce nonuniform configurations.

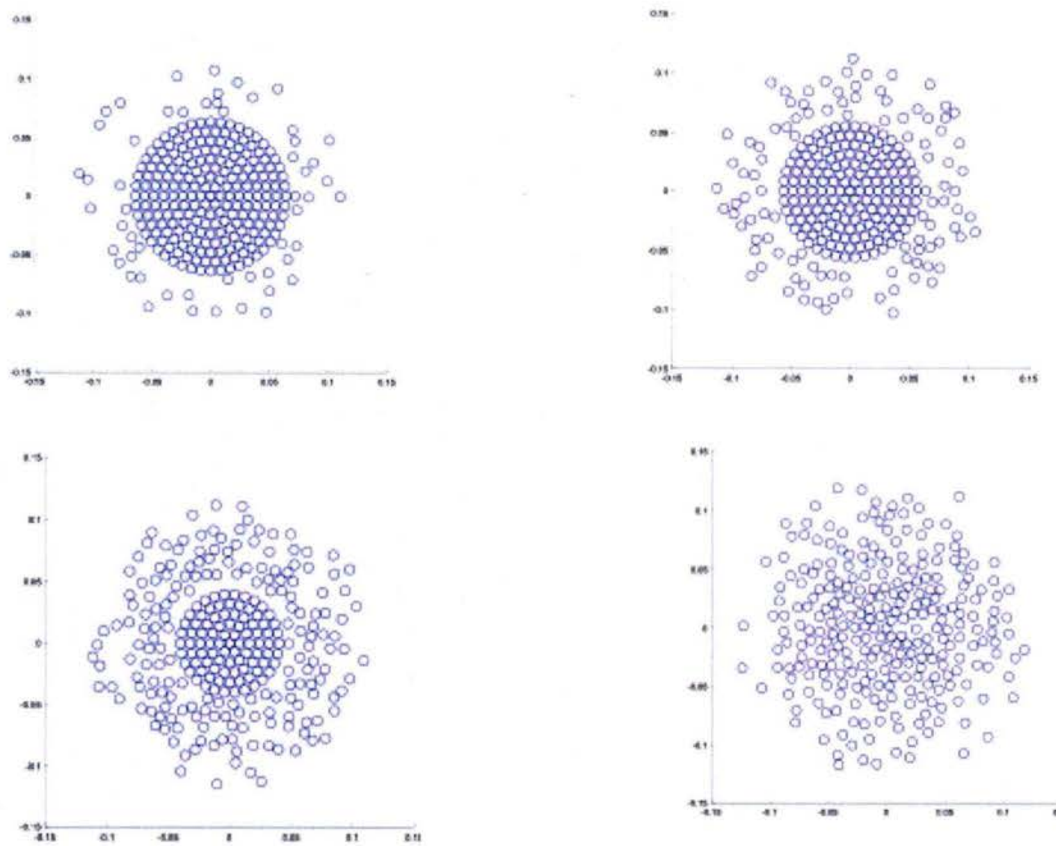

Fig. 1.2. The figure illustrates the stages in the generation of a nonuniform fiber distribution. The botto right figure is the final configuration of fibers.

As seen in Fig. 1.2, the final realization of the nonuniformly distributed fibers contains clustered regions of fibers surrounded by resin-rich areas. Each of the five realizations simulate by the procedure was analyzed by a finite element method to find the first location where dilatation driven cavitation will cause fiber-matrix debonding. Fig. 1.3 shows such a location.

It was found that for a given fiber volume fraction in a composite, a more clustered region of fibers (i.e. for smaller range of variation of the radial distance r), initiates debonding earlier (at lower applied strain).

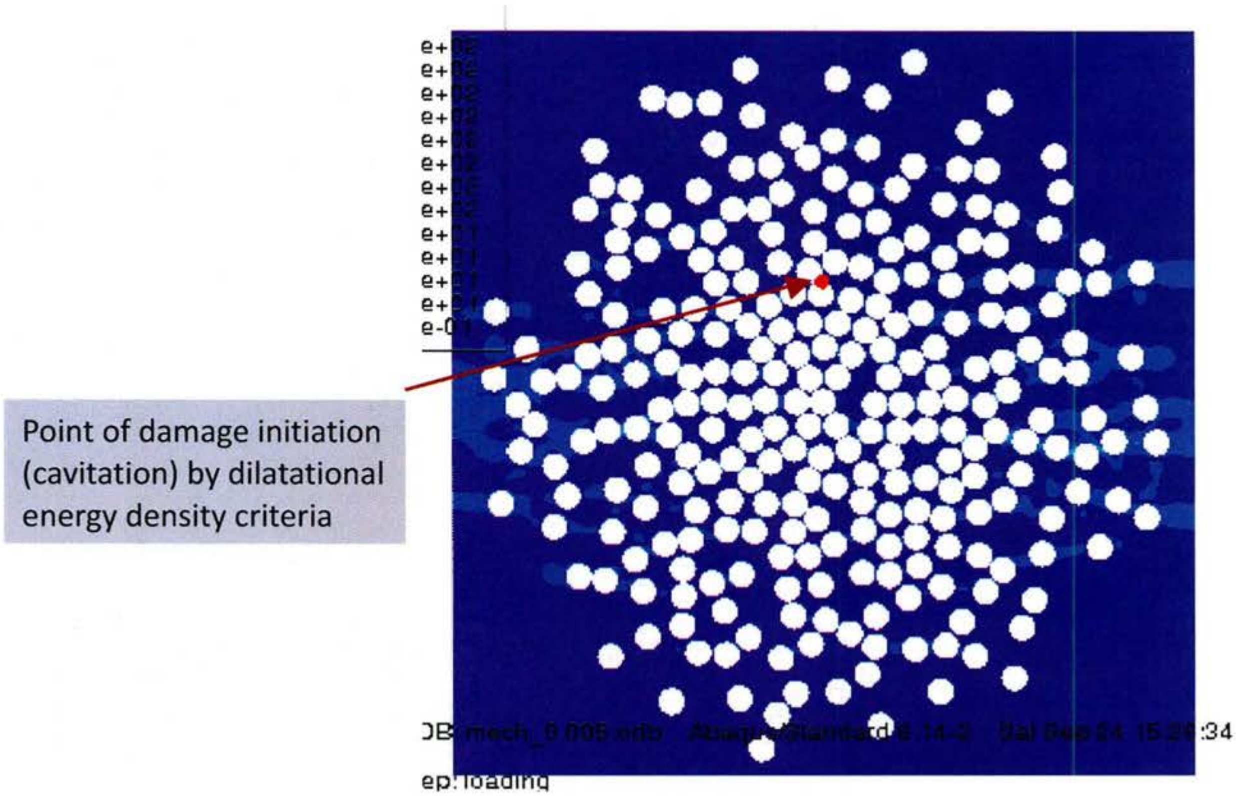

Fig. 1.3. The critical point at which debonding initiated in a realization of nonuniform (clustered fibers) fiber distribution is illustrated in this figure.

Table 1.1 summarizes the results obtained so far. As seen in the table, for the lowest range of radial variation, i.e. for the most clustered fiber configuration, the debonding initiates earliest, i.e., at the lowest applied strain. As the fibers are spread out more, the debonding becomes less likely. At the largest radial variation range, not all realizations produced dilatation and a higher strain had to be applied to get debonding in the realizations that showed debonding.

Ongoing work

Other manufacturing defects such as voids will be considered, and other loading modes than the uniaxial tension will be introduced.

Sl No	Radial variation	Rotational Variation (degrees)	No of Realizations	No of Realizations showing dilatational failure initiation	Strain range (in %)
1	±0.5r	15^0	5	2	0.6-0.65
2	±0.4r	15	5	4	0.4-0.6
3	±0.3r	15	5	5	0.3-0.4
4	±0.25r	15	5	4	0.3-0.4

Table 1.1. The table shows the average results of five realizations of the simulated fiber configurations for each case. Four cases are shown, each with a different range of the radial distance r. The rotational range is kept constant at 15^0.

Task 2.1 Peridynamic modeling of fracture and damage in materials with voids (poroelastic materials)

Motivation and Objectives

Pores, manufacturing defects, holes and round notches are locations where fatigue cracks may initiate or arrest, depending on the loading conditions. We introduce a new peridynamic model for materials with pores based on an Intermediate Homogenization Model (IHM). We investigate how the new model compares with the classical homogenization approach for dynamic elasticity as well as for crack and damage evolution. This model will allow us to model pores, voids, manufacturing defects in a composite material without having to represent the exact shape and size of such defects, which would require a very costly, fine discretization for computing the solution.

Approach and Results

Instead of following the classical approach used by homogenization approaches that work well for elasticity problems, we propose to model porosity by performing an Intermediate Homogenization (IH) step that works as follows: peridynamic (PD) bonds attached to a node are broken, randomly, up to a certain percentage that is computed based on the target porosity of the given material. To perform this step and end up with a material that has the same effective modulus as that of a given material with a given porosity P and know critical porosity P_C, we use the relationships developed in the classical damage mechanics theory (see, e.g. [1]): the effective elastic modulus of a material that has a damage index of D is proportional to (1-D). Knowing the relationship between the effective elastic modulus and the porosity of a material, we introduce a peridynamic "pre-damage" at every node of the following form:

$$\boldsymbol{d_{\mathrm{PD}} = 1 - (1 - P / P_C)^2}$$

where $\boldsymbol{d_{\mathrm{PD}}}$ is the peridynamic pre-damage index equal to the number of pre-broken bonds by the number of original bonds at that node.

We test this model to verify that the effective elastic modulus matches the one from the classical theory for poroelastic materials by sending waves and measuring their propagation speed. We then back-calculate the effective modulus given by the IH peridynamic (IHPD) model. The results are shown in Figure 2.1.

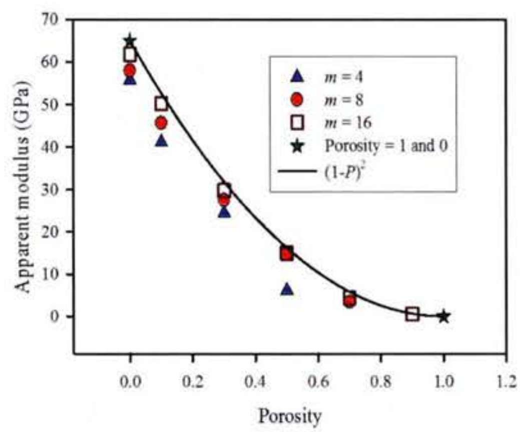

Figure 2.1. The apparent modulus versus porosity for a IHPD model computed with different m-ratios (m=horizon size divide by the grid spacing). Notice that the results converge to the classical relationship for poroelastic materials.

The benefit of using the IHPD model compared with the classical homogenization-based approach for poroelastic materials is seen when dealing with nonlinear phenomena, like material damage and fracture. This is shown next.

We consider a benchmark problem from [2]. A Berea Sandstone sample shown in Figure 2.2, is simulated with the new model. Two types of samples are in a three-point bending loading configuration: the first sample has a short notch, asymmetrically positioned about the center of the plate, while the second sample has a long notch, at the same location.

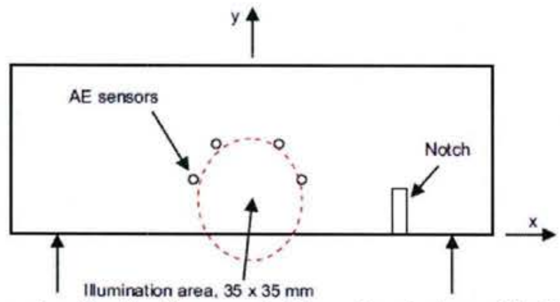

Figure 2.2. Sample geometry for the three-point bending test used in the experiments shown in [2].

The two types of samples have different failure modes: the first one fails by a crack that initiates from the center of the beam (on the bottom side), while the sample with the longer notch fails by a fracture that initiates at the notch and propagates at an angle smaller than 45 with the vertical direction (see Fig. 2.3).

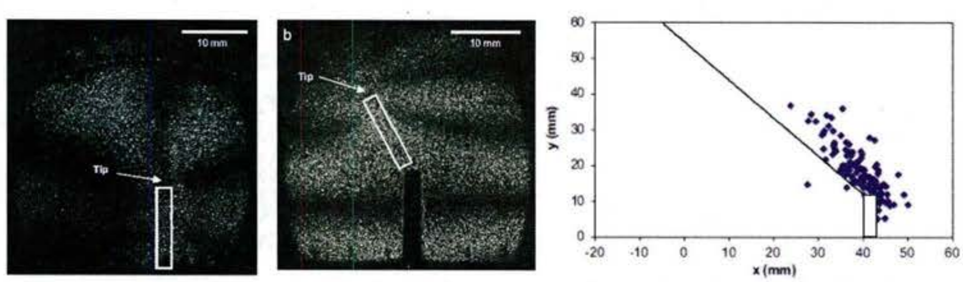

Figure 2.3. Location of the crack tips for the two types of samples (from [2]). The figure on the right shows the locations for the acoustic emissions of localized failure measured in the experiments in [2].

The peridynamic 2D model corresponding to this geometry, and using plane stress conditions, gives the results shown in Fig. 2.4.

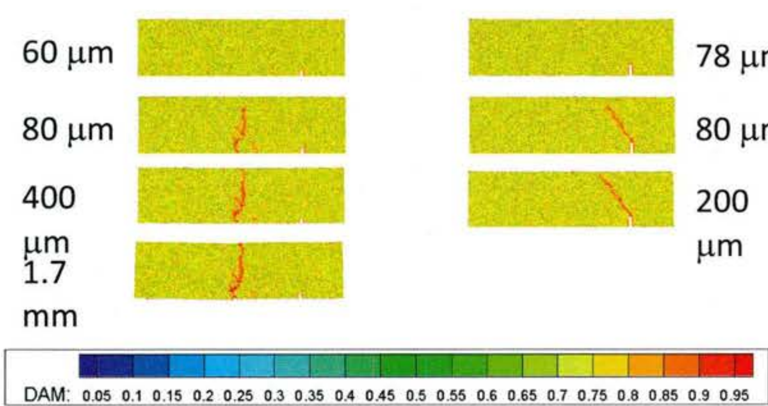

Figure 2.4. PD results for the sample with short notch (left) and sample with long notch (right). The numbers shown are the values for the imposed displacement at the top center of the plate in the three-point bending loading configuration.

We observe that the PD model confirms the results observed in the experiments. More importantly, the IHPD behaves differently, and more realistically, in terms of the fracture evolution in the porous material. Whereas with a classical type of homogenization, the fracture evolves as a single, localized crack, with the IHPD model the failure is progressive and can spread to nearby zones, as the case would be with a porous material.

Work in Progress
A publication is currently in the works based on these preliminary results. We will transfer this model to the FRC PD model in the next few months.

REFERENCES

[1] Lemaitre, J. (2012). *A course on damage mechanics*. Springer Science & Business Media.

[2] Lin, Q., Fakhimi, A., Haggerty, M., & Labuz, J. F. (2009). Initiation of tensile and mixed-mode fracture in sandstone. International Journal of Rock Mechanics & Mining Sciences, 46, 489-497.